



Differentiation of benign, intermediate, and malignant soft-tissue tumours by using multiple diffusion-weighted imaging models

K. Zhang^{a,#}, Y. Dai^{a,b,#}, C. Yu^{a,#}, J. Liu^a, Y. Cheng^a, Y. Zhou^a, Y. Liu^a, J. Tao^c, L. Zhang^d, S. Wang^{a,*}

^a Department of Radiology, The Second Hospital, Dalian Medical University, Dalian, China

^b Department of Radiology, Dalian Municipal Central Hospital, Dalian, China

^c Department of Pathology, The Second Hospital, Dalian Medical University, Dalian, China

^d Department of Radiology, The First Affiliated Hospital, Dalian Medical University, Dalian, China

ARTICLE INFORMATION

Article history:

Received 10 December 2024

Received in revised form

11 April 2025

Accepted 19 April 2025

AIM: The aim of this study was to determine whether intravoxel incoherent motion (IVIM) and diffusion kurtosis imaging (DKI) can differentiate benign, intermediate, and malignant soft-tissue tumours (STTs) of the extremities and trunk.

MATERIALS AND METHODS: We prospectively recruited 100 STT patients (32, 15, and 53 patients with benign, intermediate, and malignant tumours, respectively). The patients underwent IVIM and DKI, and the following parameters were measured: standard apparent diffusion coefficient (ADC), perfusion fraction (f), true diffusion coefficient (D_{slow}), pseudo-diffusion coefficient (D_{fast}), water diffusion heterogeneity index (α), distributed diffusion coefficient (DDC), mean diffusivity (MD), and mean kurtosis (MK). Statistical analyses were performed using receiver operating characteristic curves, the Kruskal-Wallis H test, and post hoc test with Bonferroni correction.

RESULTS: Standard ADC, D_{slow} , DDC, and MD values gradually decreased from benign to intermediate and malignant STTs. Intermediate STTs displayed a lower f value than benign tumours ($P=0.029$). The MK value was higher in malignant tumours than in intermediate and benign tumours ($P=0.021$ and <0.001 , respectively). The DDC value best differentiated benign tumours from nonbenign (intermediate and malignant) tumours (area under the curve [AUC] = 0.884, 0.853, and 0.892, respectively). The optimal MK cut-off value for differentiating intermediate and malignant tumours was 0.65 (sensitivity: 73.33%, specificity: 81.13%, accuracy: 79.41%).

CONCLUSION: IVIM and DKI parameters were helpful for differentiating benign, intermediate, and malignant STTs and can complement conventional MRI, with DDC and MK values showing high diagnostic efficacy.

© 2025 The Royal College of Radiologists. Published by Elsevier Ltd. All rights are reserved, including those for text and data mining, AI training, and similar technologies.

* Guarantor and correspondent: S. Wang, The Second Hospital of Dalian Medical University, Dalian city, Liaoning province, China.

E-mail address: wsw_2018@163.com (S. Wang).

These authors contributed equally to this work.

<https://doi.org/10.1016/j.crad.2025.106942>

0009-9260/© 2025 The Royal College of Radiologists. Published by Elsevier Ltd. All rights are reserved, including those for text and data mining, AI training, and similar technologies.

Introduction

Soft-tissue tumours (STTs) are categorised into benign, intermediate, and malignant lesions under the 2020 World Health Organization (WHO) classification of STTs (5th edition).¹ Intermediate STTs range from clinically benign lesions to highly aggressive malignancies. For patients with STTs, good clinical outcomes rely on an early and accurate diagnosis followed by timely and adequate treatments.² Currently, the preoperative diagnosis of STTs is achieved using core needle biopsy, but factors such as inexperienced operators, high tumour heterogeneity, and limited sample collection can lead to misdiagnosis, thus resulting in inappropriate treatment, especially for patients with intermediate and malignant tumours.³

Studies have indicated that conventional magnetic resonance imaging (MRI) findings, such as deep tumour location, heterogeneity, infiltrating margin, and peritumoral enhancement or oedema are associated with malignant STTs.^{4–6} The tumour size and the ratio of the axial and lateral diameter (R_{ald}) of STTs can also facilitate the discrimination of malignant, intermediate, and benign STTs,⁷ yet conventional MRI only displays morphological data and enhancement features of tumours. Different types of STTs have overlapping radiological manifestations, especially intermediate tumours that lack specific signs, making accurate differential diagnosis challenging.

Functional MRI with multiple quantitative parameters has been used to noninvasively identify the histological features and metabolic characteristics of STTs.^{8–10} Apparent diffusion coefficient (ADC) values calculated using the monoexponential model of diffusion-weighted imaging (DWI) are insufficient for the differential diagnosis of STTs; these values reflect both the diffusion of water molecules and the capillary microcirculation.^{10–14} Intravoxel incoherent motion (IVIM), an advanced DWI technique, can simultaneously estimate diffusion and perfusion parameters via the biexponential model,¹⁵ whilst the stretched-exponential model of IVIM quantifies tissue heterogeneity.¹⁶ Diffusion kurtosis imaging (DKI) assesses non-Gaussian diffusion at ultrahigh b values to characterise tumour complexity and heterogeneity.¹⁷

Both DKI and IVIM have been used for the diagnosis of breast,¹⁸ parotid gland,¹⁹ pancreas,²⁰ and ovarian tumours.²¹ Studies on distinguishing benign STTs from malignant STTs have evaluated the biexponential model of IVIM,^{22,23} but the results show evident discrepancies across studies. Moreover, most studies ignored intermediate STTs, which is not conducive to the precise treatment of patients. In addition, few studies have explored whether the stretched-exponential model of IVIM and DKI can differentiate amongst benign, intermediate, and malignant STTs.

Therefore, we comprehensively investigated the utility of IVIM and DKI for the preoperative differentiation of benign vs intermediate vs malignant STTs in the extremities and trunk.

Materials and methods

This prospective study received ethical approval from our institutional review board. We obtained written informed consent from all participants prior to the commencement of this study.

Patients

Between January 2019 and March 2024, a total of 194 patients with suspected STTs underwent multiple MRI examinations, which included IVIM and DKI sequences. Of them, 94 patients were excluded according to the following exclusion criteria: (1) no pathological confirmation; (2) non-neoplastic lesions; (3) bone tumours with large soft-tissue components; (4) poor quality of images; (5) invasive treatment prior to MRI; (6) simple lipoma; (7) tumour diameter measuring <1 cm; and (8) tumours with mainly cystic components. A flowchart of patient selection is depicted in Figure 1.

MRI sequences

All MRI sequences were acquired using a 3.0-T device (Discovery MR750w, GE HealthCare) equipped with variable coils (body, knee, or surface coil). Conventional MRI sequences included axial T1-weighted fast spin-echo (FSE) sequences (repetition time [TR]/echo time [TE]: 478-700/11-18 ms; echo train length [TEL]: 3) and fat-suppressed T2-weighted FSE sequences (TR/TE: 2900-3800/70-90 ms; TEL: 19). The following parameters were common for both sequences: slice thickness: 3 mm; slice gap: 1 mm; matrix, 384 × 384; field of view (FOV): 250 to 500 mm; and the number of excitations (NEX): 2. Sagittal and coronal fat-suppressed T1- and T2-weighted sequences were acquired after considering the location and shape of the lesion. DWI was performed using spin-echo echo-planar imaging (SE-EPI) sequences before acquiring contrast-enhanced T1-weighted sequences. The FOV, slice gap, and slice thickness for SE-EPI were identical to those used for the conventional MRI sequences. The IVIM parameters were as follows: TR/TE: 3000/70 ms; b values: 0, 25, 50, 75, 100, 200, 500, and 800 s/mm²; matrix: 128 × 128; NEX: 2 to 4; and scan time: 153 s. The DKI parameters were as follows: TR/TE: 5000/80 ms; b values: 0, 1000, and 2000 s/mm²; matrix: 128 × 128; NEX: 4; number of directions: 15; and scan time: 530 s.

Quantitative MRI analysis

DKI and IVIM scans were postprocessed using DKI and MADC software, respectively, on an Advantage Workstation (ADW 4.7, GE HealthCare). Quantitative parameters were calculated using the following formulae:

For the monoexponential model, we used the equation

$$S(b) = S_0 \cdot \exp(-b \cdot \text{ADC})$$

where b and $S(b)$ are the diffusion sensitivity coefficient and the signal intensity based on the b value, respectively.

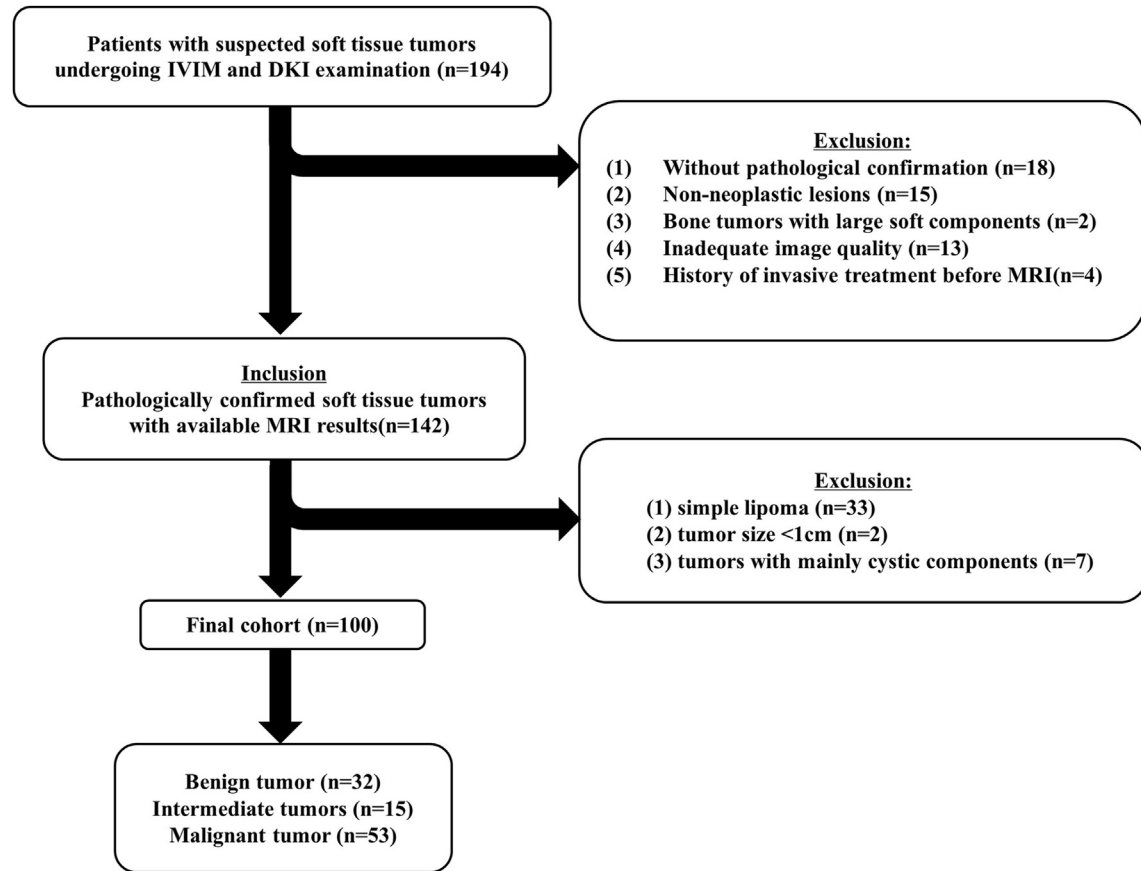


Figure 1 Study flowchart. DKI, diffusion kurtosis imaging; IVIM, intravoxel incoherent motion; MRI, magnetic resonance imaging.

For the biexponential model, we used the equation

$$S(b) = S_0 \cdot [f \cdot \exp(b \cdot D_{\text{fast}}) + (1 - f) \cdot \exp(-b \cdot D_{\text{slow}})]$$

where D_{slow} , D_{fast} , and f are the true diffusion coefficient, pseudo-diffusion coefficient, and perfusion fraction, respectively.¹⁵

For the stretched-exponential model, we used the equation

$$S(b) = S_0 \cdot \exp[-(b \cdot \text{DDC})^\alpha]$$

where DDC is the distributed diffusion coefficient representing the continuous distribution of diffusion coefficients within voxels and α is the water diffusion heterogeneity index representing the deviation of water-molecule diffusion from the monoexponential model.¹⁶ The α value is bound between 0 and 1.

For DKI, we used the equation

$$S(b) = S_0 \cdot \exp.(-b \cdot D_{\text{app}} + b^2 \cdot D_{\text{app}}^2 \cdot K_{\text{app}}/6)$$

where K_{app} and D_{app} represent distribution kurtosis- and the ADC-corrected values for non-Gaussian diffusion, respectively. We calculated the mean kurtosis (MK) and mean diffusivity (MD) for 15 directions.¹⁷

Regions of interest (ROIs) were placed on the ADC maps by 2 radiologists (with 7 and 17 years of experience) who were blinded to the clinicopathological data. T1-weighted,

T2-weighted, and contrast-enhanced images served as references for ROI placement. Each ROI contained the largest solid portion of each tumour and avoided areas of haemorrhage, necrosis, cystic changes, and oedema as well as tumour margins and gross artifacts. The 2 examiners' measurements were averaged and used for statistical analysis.

Qualitative MRI analysis

The 2 radiologists independently recorded the subsequent conventional MRI signs for each tumour: tumour size, R_{ald} , tissue layer, margin characteristics, necrosis, tumour heterogeneity on T2-weighted images, peritumoral oedema and enhancement, and invasion of the bones, vessels, or nerves. The precise definitions of the above features are provided in [Supplementary Material S1](#).

Histopathological evaluation

Histopathological diagnoses were independently performed by 2 pathologists (with 5 and 15 years of experience) in a blinded manner. Any disagreements between the 2 pathologists were resolved by consultation with a third pathologist with 20 years of experience. On histological examination, all STTs were divided into benign, intermediate, or malignant lesions according to the 2020 WHO classification.

Statistical analysis

Statistical analyses were conducted using MedCalc v15.8 (Mariakerke, Belgium) and SPSS v25.0 (Chicago, USA) software. The normality of data and homogeneity of variance were assessed using the Kolmogorov-Smirnov and Levene tests, respectively. All normally distributed data were expressed as mean \pm standard deviation; data that did not conform to a normal distribution were expressed as median (interquartile range). Categorical and quantitative variables were compared amongst the 3 STT types by using the chi-squared test and Kruskal-Wallis H test, respectively. Post hoc analysis was performed using the Dunn's test with the Bonferroni correction for pairwise comparisons. Interexaminer agreement was assessed using intraclass correlation coefficients (ICCs), with ICCs >0.75 indicating good agreement. The receiver operating characteristic (ROC) curve and area under the curve (AUC) were used to determine the diagnostic performance of quantitative parameters, and their optimal cut-off values, sensitivity, specificity, and accuracy were calculated using the Youden's index. Multivariable logistic regression analysis was performed to evaluate diffusion parameters. AUCs were evaluated using the DeLong test. Differences were deemed significant at a P value <0.05 .

Results

General information

The study involved 100 patients, of whom 5 patients were unable to undergo contrast-enhanced examinations due to contraindications. According to the pathological results of surgical resection, 100 patients were divided into 3 groups: benign STTs ($n=32$), intermediate STTs ($n=15$), and malignant STTs ($n=53$). The tumour type was not related to

gender; however, the degree of malignancy was found to increase with increasing age, which is consistent with the epidemiological characteristics of STTs (Table 1). The study consisted of 48 male patients and 52 female patients. The mean age of the patients was 55 years (range: 12-85 years). The most frequently involved anatomical location was the thigh ($n=32$), followed by the trunk ($n=18$), distal lower limb ($n=17$), upper limb ($n=17$), hip ($n=8$), shoulder ($n=7$), and hand ($n=1$).

Conventional MRI findings

The conventional MRI features examined are presented in Table 2 and Supplementary Material Table 1. We found that tumour size, necrosis, T2-weighted heterogeneity, and peritumoral oedema all significantly differed amongst benign, intermediate, and malignant STTs. Pairwise comparisons revealed that compared to benign STTs, malignant STTs were significantly larger (mean: 7.15 vs 4.33 cm; $P=0.001$) and more frequently associated with necrosis ($P=0.012$), heterogeneity ($P=0.017$), and peritumoral oedema ($P=0.006$). The AUCs of tumour size, necrosis, T2-weighted heterogeneity, and peritumoral oedema for distinguishing between benign and malignant STTs were 0.752, 0.629, 0.597, and 0.676, respectively. However, intermediate STTs did not differ from benign and malignant tumours in terms of the 4 aforementioned parameters ($P>0.05$).

Interexaminer agreement

Good interexaminer agreement was observed for all parameters (ICCs: 0.788-0.974), except for D_{fast} (ICC = 0.660) and f (ICC = 0.604; Table 3).

Table 1
Demographic data and tumour characteristics.

	Benign (n=32)	Intermediate (n=15)	Malignant (n=53)	P value
Age (year)	48.73 \pm 15.52	49.07 \pm 15.21	59.79 \pm 18.77	0.004
Gender	F:M = 18:14	F:M = 11:4	F:M = 23:30	0.103
Histological diagnosis	Neurofibroma (n=6) Schwannoma (n=7) GCTTS (n=7) Intramuscular myxoma (n=1) Nodular fasciitis (n=1) Haemangioma (n=7) Benign fibrous histiocytoma (n=2) Pilomatricoma (n=1)	Dermatofibrosarcoma protuberans (n=6) Atypical lipomatous tumour (n=3) Inflammatory myofibroblastic tumour (n=1) Desmoid-type fibromatosis (n=4) Solitary fibrous tumour (n=1)	Dedifferentiated liposarcoma (n=2) Pleomorphic liposarcoma (n=4) Myxoid liposarcoma (n=6) Fibrosarcoma (n=4) Synovial sarcoma (n=7) Leiomyosarcoma (n=10) UPS (n=6) MPNST (n=4) MGCTS (n=1) Angiosarcoma (n=2) Alveolar soft part sarcoma (n=1) Rhabdomyosarcoma (n=2) Extraskeletal myxoid chondrosarcoma (n=1) Lymphoma (n=3)	

F, female; GCTTS, giant cell tumour of tendon sheath; M, male; MGCTS, malignant giant cell tumour of tendon sheath; MPNST, malignant peripheral nerve sheath tumour; UPS, undifferentiated pleomorphic sarcoma.

Table 2
Conventional MRI features of soft-tissue tumours.

Parameters	Benign (n=29)	Intermediate (n=15)	Malignant (n=51)	P value
Tumour size (cm)	4.33 ± 2.68	5.29 ± 1.84	7.15 ± 4.04	0.002
R _{ald}	0.634 ± 0.142	0.644 ± 0.142	0.615 ± 0.140	0.624
Tissue layer				0.603
Deep	17/29 (58.7)	8/15 (53.3)	24/51 (47.1)	
Superficial	12/29 (41.3)	7/15 (46.7)	27/51 (52.9)	
Margin				0.367
Poorly defined	10/29 (34.4)	4/15 (26.7)	23/51 (45.1)	
Well defined	19/29 (65.6)	11/15 (73.3)	28/51 (54.9)	
Necrosis				0.026
Present	8/29 (27.6)	5/15 (33.3)	29/51 (56.9)	
Absent	21/29 (72.4)	10/15 (66.7)	22/51 (43.1)	
T2WI heterogeneity				0.042
Present	12/29 (41.4)	7/15 (46.7)	35/51 (68.6)	
Absent	17/29 (58.6)	8/15 (53.3)	16/51 (31.4)	
Peritumoral oedema				0.018
Present	9/29 (31.0)	6/15 (40.0)	32/51 (62.7)	
Absent	20/29 (67.0)	9/15 (60.0)	19/51 (37.3)	
Peritumoral enhancement				0.155
Present	7/29 (24.1)	8/15 (53.3)	18/51 (35.3)	
Absent	22/29 (75.9)	7/15 (46.7)	33/51 (64.7)	
Bone invasion				0.439
Present	2/29 (6.9)	0/15 (0.0)	5/51 (11.8)	
Absent	27/29 (93.1)	15/15 (100.0)	46/51 (80.4)	
Vessel and/or nerve invasion				0.096
Present	3/29 (10.3)	2/15 (13.3)	15/51 (29.4)	
Absent	26/29 (89.7)	13/15 (86.7)	36/51 (70.6)	

MRI, magnetic resonance imaging; R_{ald}, ratio of the axial and lateral diameter; T2WI, T2-weighted imaging.

Table 3
Interexaminer agreement for measurements of diffusion parameters.

Parameters	ICC	95% CI
Standard ADC ($\times 10^{-3}\text{mm}^2/\text{s}$)	0.900	0.855–0.931
D _{slow} ($\times 10^{-3}\text{mm}^2/\text{s}$)	0.927	0.893–0.950
D _{fast} ($\times 10^{-3}\text{mm}^2/\text{s}$)	0.660	0.753–0.758
<i>f</i>	0.604	0.463–0.715
DDC ($\times 10^{-3}\text{mm}^2/\text{s}$)	0.914	0.874–0.941
α	0.788	0.701–0.852
MK	0.974	0.961–0.982
MD ($\times 10^{-3}\text{mm}^2/\text{s}$)	0.958	0.938–0.972

α , water diffusion heterogeneity index; ADC, apparent diffusion coefficient; CI, confidence interval; DDC, distributed diffusion coefficient; D_{fast}, pseudo-diffusion coefficient; D_{slow}, true diffusion coefficient; *f*, perfusion fraction; ICC, Intraclass correlation coefficient; MD, mean diffusivity; MK, mean kurtosis.

Quantitative diffusion parameter analysis

As shown in Table 4 and Supplementary Material Table 2, the quantitative parameters standard ADC, D_{slow}, *f*, DDC, MK, and MD values significantly differed amongst benign, intermediate, and malignant STTs (*f* value: $P=0.017$, other parameters: $P<0.001$, Kruskal-Wallis H test). Standard ADC, D_{slow}, DDC, and MD values were lower in the malignant tumour group than in the benign tumour group ($P<0.001$ for all). DDC, D_{slow}, *f*, and MD values were lower in the intermediate group than in the benign group ($P=0.006$, 0.023, 0.029, and 0.038, respectively). The MK value was significantly higher in malignant STTs than in intermediate STTs ($P=0.021$) and benign STTs ($P<0.001$).

Table 4
Diffusion parameters of soft-tissue tumours.

Parameters	Benign (n=32)	Intermediate (n=15)	Malignant (n=53)	P value ^a	P value ^b		
					Benign vs intermediate	Intermediate vs malignant	Benign vs malignant
Standard ADC ($\times 10^{-3}\text{mm}^2/\text{s}$)	1.67 (1.50-1.73)	1.47 (1.37-1.55)	1.29 (1.15-1.49)	<0.001	0.120	0.173	<0.001
D _{slow} ($\times 10^{-3}\text{mm}^2/\text{s}$)	1.46 (1.38-1.58)	1.26 (1.11-1.34)	1.09 (0.94-1.21)	<0.001	0.023	0.340	<0.001
D _{fast} ($\times 10^{-3}\text{mm}^2/\text{s}$)	16.64 (10.37-35.70)	34.20 (15.10-49.95)	26.45 (17.05-32.46)	0.096			
<i>f</i>	24.65 (17.74-30.59)	20.30 (11.85-25.25)	19.15 (14.25-25.58)	0.017	0.029	0.867	0.076
DDC ($\times 10^{-3}\text{mm}^2/\text{s}$)	1.74 (1.57-1.91)	1.44 (1.29-1.54)	1.18 (1.08-1.41)	<0.001	0.006	0.383	<0.001
α	0.92 (0.82-0.96)	0.85 (0.75-0.91)	0.88 (0.82-0.92)	0.079			
MK	0.53 (0.42-0.66)	0.60 (0.56-0.73)	0.78 (0.70-0.83)	<0.001	0.604	0.021	<0.001
MD ($\times 10^{-3}\text{mm}^2/\text{s}$)	2.15 (1.95-2.24)	1.82 (1.63-1.92)	1.42 (1.25-1.87)	<0.001	0.038	0.098	<0.001

α , water diffusion heterogeneity index; ADC, apparent diffusion coefficient; DDC, distributed diffusion coefficient; D_{fast}, pseudo-diffusion coefficient; D_{slow}, true diffusion coefficient; *f*, perfusion fraction; MD mean diffusivity; MK, mean kurtosis. Data are medians with interquartile ranges in parentheses. P values^a are calculated from the Kruskal-Wallis H test. P values^b are adjusted for pairwise comparisons by using the Dunn's test with the Bonferroni correction.

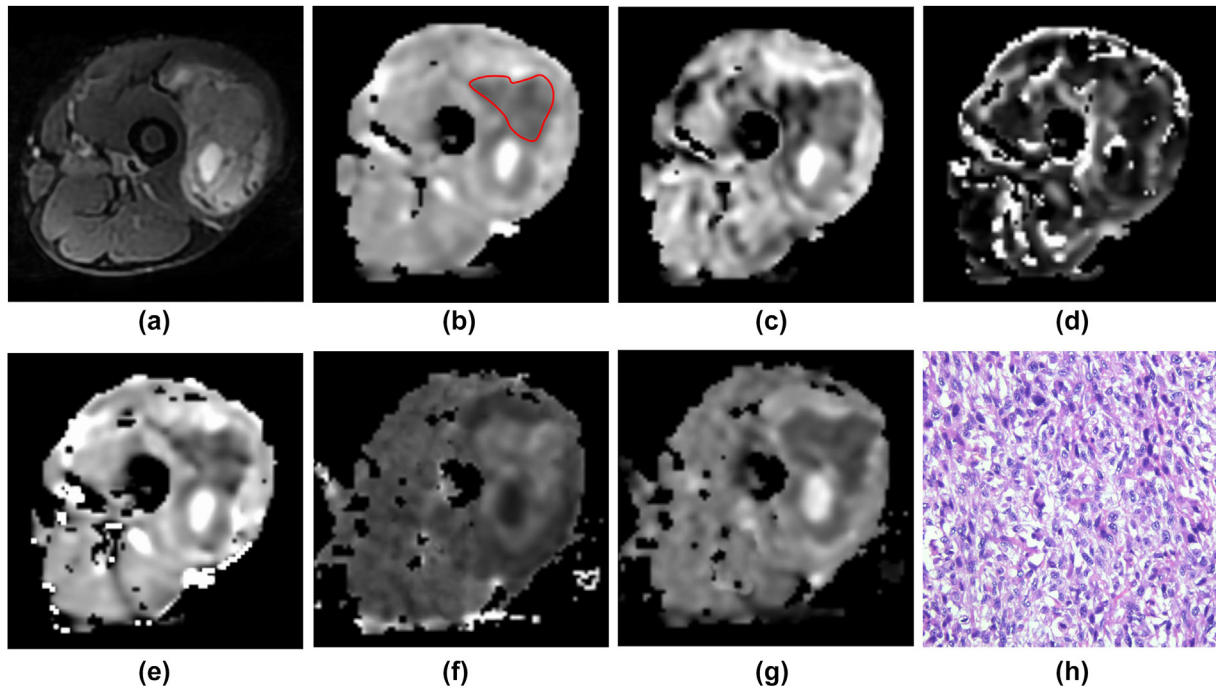


Figure 2 A 55-year-old patient with leiomyosarcoma of the left thigh. (a) Axial T2-weighted image showing a hyperintense mass with multiple cystic regions. The standard ADC (b), D_{slow} (c), f (d), DDC (e), MK (f), and MD (g) values are $1.27 \times 10^{-3} \text{ mm}^2/\text{s}$, $1.11 \times 10^{-3} \text{ mm}^2/\text{s}$, 11.90 , $1.10 \times 10^{-3} \text{ mm}^2/\text{s}$, 0.77 , and $1.58 \times 10^{-3} \text{ mm}^2/\text{s}$, respectively. (h) On microscopy, the tumour cells show a spindle-shaped or oval appearance, and are arranged in a parallel pattern with variable amounts of eosinophilic cytoplasm and vesicular nuclei (haematoxylin and eosin, $\times 200$ original magnification). ADC, apparent diffusion coefficient; DDC, distributed diffusion coefficient; D_{slow} , true diffusion coefficient; f , perfusion fraction; MD, mean diffusivity; MK, mean kurtosis.

The conventional MRI and diffusion characteristics of histologically confirmed cases of leiomyosarcoma, dermatofibrosarcoma protuberans, and neurofibroma are shown in [Figure 2](#), [Supplementary Material Figure S1](#), and [Figure S2](#), respectively.

Diagnostic performance

The diagnostic performance of quantitative diffusion parameters is illustrated in [Table 5](#) and [Figure 3](#).

For differentiating benign tumours from intermediate tumours, DDC value showed the highest AUC (0.853);

Table 5
Performance of quantitative imaging parameters for diagnosing soft-tissue tumours.

Parameters	AUC	95% CI	Cut-off value	Youden's index	Sensitivity (%)	Specificity (%)	Accuracy (%)
Benign vs intermediate							
D_{slow} ($\times 10^{-3} \text{ mm}^2/\text{s}$)	0.820	0.680–0.917	>1.34	0.581	78.1 (25/32)	80.0 (12/15)	78.7 (37/47)
f	0.725	0.575–0.845	>26.05	0.406	40.6 (13/32)	100.0 (15/15)	59.6 (28/47)
DDC ($\times 10^{-3} \text{ mm}^2/\text{s}$)	0.853	0.719–0.939	>1.63	0.621	68.8 (22/32)	93.3 (14/15)	76.6 (36/47)
MD ($\times 10^{-3} \text{ mm}^2/\text{s}$)	0.803	0.661–0.905	>2.07	0.590	65.6 (21/32)	93.3 (14/15)	74.5 (35/47)
Combination of 4 parameters	0.900	0.777–0.968	/	0.777	84.4 (27/32)	93.3 (14/15)	83.0 (39/47)
Benign vs malignant							
Standard ADC ($\times 10^{-3} \text{ mm}^2/\text{s}$)	0.829	0.732–0.902	>1.49	0.586	81.3 (26/32)	77.4 (41/53)	78.8 (67/85)
D_{slow} ($\times 10^{-3} \text{ mm}^2/\text{s}$)	0.855	0.762–0.922	>1.21	0.680	90.6 (30/32)	77.4 (41/53)	83.5 (71/85)
DDC ($\times 10^{-3} \text{ mm}^2/\text{s}$)	0.892	0.806–0.949	>1.51	0.712	84.4 (27/32)	86.8 (46/53)	85.9 (73/85)
MK	0.822	0.724–0.897	≤ 0.67	0.624	81.3 (26/32)	81.1 (43/53)	81.2 (69/85)
MD ($\times 10^{-3} \text{ mm}^2/\text{s}$)	0.886	0.798–0.944	>2.01	0.656	75.0 (24/32)	90.6 (48/53)	84.7 (72/85)
Combination of 5 parameters	0.920	0.841–0.968	/	0.793	90.6 (29/32)	88.7 (47/53)	87.1 (74/85)
Intermediate vs malignant							
MK	0.778	0.661–0.870	≤ 0.65	0.545	73.3 (11/15)	81.1 (43/53)	79.4 (54/68)
Benign vs nonbenign (intermediate + malignant)							
D_{slow} ($\times 10^{-3} \text{ mm}^2/\text{s}$)	0.847	0.761–0.911	>1.34	0.634	78.1 (25/32)	85.3 (58/68)	83.0 (83/100)
DDC ($\times 10^{-3} \text{ mm}^2/\text{s}$)	0.884	0.804–0.939	>1.52	0.682	84.4 (27/32)	85.3 (58/68)	85.0 (85/100)
MD ($\times 10^{-3} \text{ mm}^2/\text{s}$)	0.867	0.785–0.927	>2.01	0.632	75.0 (24/32)	88.2 (60/68)	84.0 (84/100)
Combination of 3 parameters	0.916	0.843–0.962	/	0.790	93.8 (30/32)	85.3 (58/68)	88.0 (88/100)

ADC, apparent diffusion coefficient; AUC, area under the curve; CI, confidence interval; DDC, distributed diffusion coefficient; D_{slow} , true diffusion coefficient; f , perfusion fraction; MD, mean diffusivity; MK, mean kurtosis.

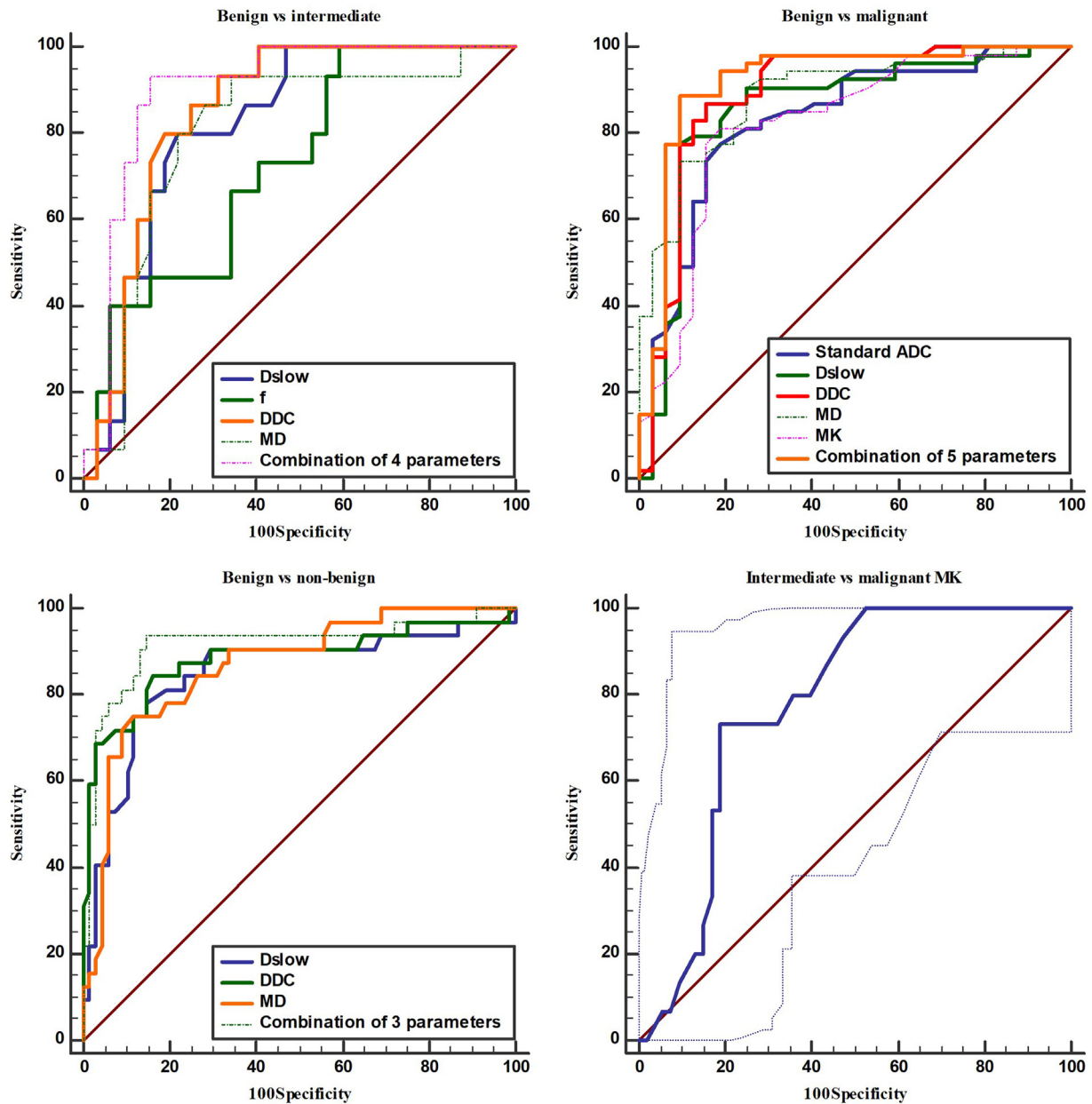


Figure 3 ROC curves showing the diagnostic performance of quantitative imaging parameters for differentiating soft-tissue tumours. DDC, distributed diffusion coefficient; MD, mean diffusivity; MK, mean kurtosis.

however, the AUC for DDC value did not significantly differ from those for D_{slow} , f , and MD values ($P=0.522$, 0.146 , and 0.494 , respectively). A combination of D_{slow} , f , DDC, and MD yielded to an AUC of 0.900 with a sensitivity of 84.37% and a specificity of 93.33%. The AUC of the combined model was higher than those of the f and MD values (0.900 vs 0.725 and 0.803 , $P=0.011$ and 0.047 , respectively) but did not significantly differ from those of the D_{slow} and DDC values ($P=0.122$ and 0.147 , respectively).

For discriminating between benign and malignant STTs, the AUC of DDC value was higher than that of tumour size (0.892 vs 0.725 , $P=0.027$), but the AUC of DDC value did not significantly differ from those of standard ADC, D_{slow} , MK, and MD values ($P=0.060$, 0.232 , 0.112 , and 0.866 ,

respectively). The combination of standard ADC, D_{slow} , DDC, MK, and MD values yielded an AUC of 0.920, a sensitivity of 90.62%, and a specificity of 88.68%. The AUC of this combined model was higher than those of the standard ADC, D_{slow} , and MK values (0.920 vs 0.829 , 0.855 , and 0.822 , $P=0.017$, 0.028 , and 0.007 , respectively) but did not differ from those of the DDC and MD values ($P=0.190$ and 0.188 , respectively).

For the discrimination of intermediate vs malignant STTs, the optimal cut-off MK value was 0.65 (sensitivity: 73.33%, specificity: 81.13%, and accuracy: 79.41%).

The D_{slow} , DDC, and MD values of benign tumours significantly differed from those of intermediate and malignant tumours; hence, the latter 2 groups were combined

as the nonbenign group for further analysis. The D_{slow} , DDC, and MD values helped discriminate benign STTs from nonbenign STTs (Table 5), with DDC value showing the highest AUC (0.884). However, the AUC of DDC value did not significantly differ from those of D_{slow} and MD values ($P=0.261$ and 0.689 , respectively). A combination of D_{slow} , DDC, and MD yielded to an AUC of 0.916 with a sensitivity of 93.75% and a specificity of 85.29%. The AUC of the combined model was higher than that of the D_{slow} value (0.916 vs 0.847, $P=0.018$) but did not differ from those of the DDC and MD values ($P=0.143$ and 0.077 , respectively).

Discussion

The findings of our study indicated that IVIM- and DKI-derived quantitative parameters can reveal the diffusion and perfusion characteristics of STTs. We then developed a preliminary stepwise diagnostic diagram to distinguish between benign, intermediate, and malignant STTs.

Conventional MRI is commonly used to diagnose STTs, and malignant STTs usually demonstrate a more aggressive growth pattern on MRI. We found that tumour size, necrosis, T2-weighted heterogeneity, and peritumoral oedema could differentiate benign STTs from malignant STTs, which is in agreement with published findings.^{5,12,24} However, these features could not distinguish intermediate tumours from benign or malignant tumours. Peritumoral enhancement is associated with malignant tumours due to their increased vascularity⁴; however, we found no significant difference in peritumoral enhancement amongst the 3 types of STTs. In addition, unlike the findings of Gruber *et al.*,⁷ we found no significant difference in R_{ald} , which may be related to the multiple anatomical locations of the included tumours. These results highlight the limitations of conventional MRI in the differentiation of STT types.

Standard ADC, D_{slow} , DDC, and MD values all reflect restricted water diffusion in tissues and are primarily affected by cell density.^{25,26} Consistent with previous studies,^{27–29} our study showed that all 4 types of ADC values gradually declined from benign to nonbenign (intermediate and malignant) tumours. D_{slow} , DDC, and MD values could distinguish benign tumours from intermediate and malignant tumours. Malignant tumour cells tend to exhibit abundant growth and a dense distribution, which reduces the extracellular space and thereby decreases the ADC. The DDC value is a composite of individual ADC values across different distributions and directions, and theoretically reflects water-molecule diffusion more accurately than ADC.¹⁶ Few studies have examined the usefulness of DDC in the diagnosis of STTs. In the present study, the DDC value showed the best diagnostic performance in differentiating benign STTs from non-benign STTs, which is inconsistent with the findings obtained in endometrial lesions.²⁵ This difference may be attributable to the difference in tumour types.

We found that the D_{fast} value was higher in intermediate STTs than in benign and malignant STTs, although the

differences were not significant. In contrast, the f value was significantly lower in intermediate STTs than in benign STTs, which is consistent with a previous report.²² This finding suggests that benign STTs have more intact capillaries than intermediate STTs. As important perfusion parameters reflecting capillary microcirculation, the repeatability of D_{fast} and f has always been controversial.³⁰ Wu *et al.*²² reported a higher D_{fast} value and a similar f value in malignant STTs as compared to those in benign STTs, and Lim *et al.*³¹ reported the opposite results. The discrepancy may be attributable to the fact that the combination of b values used is critical for IVIM-derived parameters as too few b values measuring below 100 to 200 s/mm² (range for perfusion sensitivity) will reduce the performance of perfusion parameters.³² Another explanation may be that different tumour subtypes have varying degrees of vascularisation and cell density.

During the malignant transformation of tumours, the tumour microstructure becomes more complex and diverse, potentially altering the motion of water molecules. Both α and MK values can indicate the intravoxel heterogeneity of water diffusion; increased tumour heterogeneity is associated with reduced α values and increased MK. In a prospective study by Ogawa *et al.* that assessed the value of MK in the differential diagnosis of musculoskeletal tumours, a significant difference was found between the MK values of benign and malignant tumours.³³ In our study, we similarly found a significant difference in MK values between benign and malignant STTs. Malignant tumours exhibit cellular pleomorphism, necrosis, haemorrhage, and tortuous vascular hyperplasia, all of which influence MK values. Malignant and benign STTs did not differ in terms of α values, which is consistent with studies of endometrial²⁵ and liver lesions.³⁴ These results indicate that the MK value from the DKI model is more suitable for evaluating the tumour microenvironment than the α value from the stretched-exponential model.

Intermediate STTs are a special tumour type with diverse biological behaviours that are often misdiagnosed as benign or malignant STTs. Most studies on STTs classified the tumours into the benign and malignant categories.^{5,11,12,23,24} With the deepening of the concept of precision medicine, intermediate tumours are receiving increasing attention from clinicians, imaging physicians, and pathologists,^{3,35} and distinguishing intermediate from benign and malignant tumours is related to improving patient management and adjusting treatment decisions. The present results confirmed that conventional MRI is insufficient to distinguish intermediate tumours from benign and malignant tumours. IVIM- and DKI-derived parameters provide diversified information. In the present study, the DDC value displayed the best diagnostic performance amongst all the other parameters examined. Logistic regression models including multiple parameters and their combinations did not show significantly higher diagnostic performance than DDC values. Additionally, only MK value could distinguish between intermediate and malignant tumours. Therefore, we consider incorporating DDC and MK values into the

differential diagnosis of STTs. In the future, we need larger sample sizes and more advanced analytical methods to optimise and validate the results of this preliminary study.

Our study has some limitations. First, the sample size was small, especially for the intermediate STT group. Therefore, our study only provided a preliminary exploratory result. Second, we used ROIs that were manually drawn in the solid tumour component rather than the whole tumour. This method may produce measurement errors in highly heterogeneous tumours. In addition, no uniform standard was available for the selection and number of b values in diffusion sequences. For the stretched-exponential model and DKI, using higher b values may result in more accurate calculation of quantitative parameters. Therefore, we need to increase the sample size, further optimise the combination of b values, and analyse the whole tumour volume to more accurately reflect the microscopic changes in STTs.

In summary, the results of the present study showed that quantitative parameters derived using IVIM and DKI perform better in the differential diagnosis of benign, intermediate, and malignant STTs than conventional MRI. The DDC values from the stretched-exponential model best differentiated benign tumours from nonbenign (intermediate/malignant) tumours. The MK values from DKI were useful for differentiating intermediate and malignant STTs.

Author contribution

1. Guarantor of integrity of the entire study: Kai Zhang and Shaowu Wang.
2. Study concepts and design: Kai Zhang and Yue Dai.
3. Literature research: Juntong Liu, Yu Cheng, and Yanyun Zhou.
4. Clinical studies: Yue Dai and Chuanwen Yu.
5. Experimental studies/data analysis: Yajie Liu and Juan Tao.
6. Statistical analysis: Kai Zhang and Lina Zhang.
7. Manuscript preparation: Kai Zhang and Chuanwen Yu.
8. Manuscript editing: Yue Dai and Shaowu Wang.

Funding

All for this research was supported by grants from the National Natural Science Foundation of China (#82271975).

Conflict of Interest

The authors declare no conflict of interest.

Acknowledgements

The authors gratefully acknowledge the financial supports by the National Natural Science Foundation of China under Grant numbers #82271975.

Appendix A. Supplementary data

Supplementary data to this article can be found online at <https://doi.org/10.1016/j.crad.2025.106942>.

References

1. Choi JH, Ro JY. The 2020 WHO classification of tumors of soft tissue: selected changes and new entities. *Adv Anat Pathol* 2020;**28**:44–58.
2. Gamboa AC, Gronchi A, Cardona K. Soft-tissue sarcoma in adults: an update on the current state of histiotype-specific management in an era of personalized medicine. *CA Cancer J Clin* 2020;**70**:200–29.
3. Yoon MA, Chung HW, Chee CG, et al. Risk factors for diagnostic failure of ultrasound-guided core needle biopsy of soft-tissue tumors based on World Health organization classification category and biologic potential. *AJR Am J Roentgenol* 2020;**214**:413–21.
4. Crombé A, Marcellin PJ, Buy X, et al. Soft-tissue sarcomas: assessment of MRI features correlating with histologic grade and patient outcome. *Radiology* 2019;**291**:710–21.
5. Choi YJ, Lee IS, Song YS, et al. Diagnostic performance of diffusion-weighted (DWI) and dynamic contrast-enhanced (DCE) MRI for the differentiation of benign from malignant soft-tissue tumors. *J Magn Reson Imaging* 2019;**50**:798–809.
6. Ahlawat S, Fritz J, Morris CD, et al. Magnetic resonance imaging biomarkers in musculoskeletal soft tissue tumors: review of conventional features and focus on nonmorphologic imaging. *J Magn Reson Imaging* 2019;**50**:11–27.
7. Gruber L, Loizides A, Ostermann L, et al. Does size reliably predict malignancy in soft tissue tumours? *Eur Radiol* 2016;**26**:4640–8.
8. Fayad LM, Jacobs MA, Wang X, et al. Musculoskeletal tumors: how to use anatomic, functional, and metabolic MR techniques. *Radiology* 2012;**265**:340–56.
9. Chianca V, Albano D, Messina C, et al. An update in musculoskeletal tumors: from quantitative imaging to radiomics. *Radiol Med* 2021;**126**:1095–105.
10. Dodin G, Salleron J, Jendoubi S, et al. Added-value of advanced magnetic resonance imaging to conventional morphologic analysis for the differentiation between benign and malignant non-fatty soft-tissue tumors. *Eur Radiol* 2021;**31**:1536–47.
11. Lee SY, Jee WH, Jung JY, et al. Differentiation of malignant from benign soft tissue tumours: use of additive qualitative and quantitative diffusion-weighted MR imaging to standard MR imaging at 3.0 T. *Eur Radiol* 2016;**26**:743–54.
12. Song Y, Yoon YC, Chong Y, et al. Diagnostic performance of conventional MRI parameters and apparent diffusion coefficient values in differentiating between benign and malignant soft-tissue tumours. *Clin Radiol* 2017;**72**:691.e1–691.e10.
13. Wang Q, Xiao X, Liang Y, et al. Diagnostic performance of diffusion MRI for differentiating benign and malignant nonfatty musculoskeletal soft tissue tumors: a systematic review and meta-analysis. *J Cancer* 2021;**12**:7399–412.
14. Jeon JY, Chung HW, Lee MH, et al. Usefulness of diffusion-weighted MR imaging for differentiating between benign and malignant superficial soft tissue tumours and tumour-like lesions. *Br J Radiol* 2016;**89**:20150929.
15. Le Bihan D, Breton E, Lallemand D, et al. Separation of diffusion and perfusion in intravoxel incoherent motion MR imaging. *Radiology* 1998;**168**:497–505.
16. Bennett KM, Schmainda KM, Bennett RT, et al. Characterization of continuously distributed cortical water diffusion rates with a stretched-exponential model. *Magn Reson Med* 2003;**50**:727–34.
17. Jensen J, Helpert J, Ramani A, et al. Diffusional kurtosis imaging: the quantification of non-Gaussian water diffusion by means of magnetic resonance imaging. *Magn Reson Med* 2005;**53**:1432–40.
18. Jin YN, Zhang Y, Cheng JL, et al. Monoexponential, Biexponential, and stretched-exponential models using diffusion-weighted imaging: a quantitative differentiation of breast lesions at 3.0T. *J Magn Reson Imaging* 2019;**50**:1461–7.
19. Huang N, Chen Y, She D, et al. Diffusion kurtosis imaging and dynamic contrast-enhanced MRI for the differentiation of parotid gland tumors. *Eur Radiol* 2022;**32**:2748–59.

20. Shi YJ, Li XT, Zhang XY, et al. Non-Gaussian models of 3-Tesla diffusion-weighted MRI for the differentiation of pancreatic ductal adenocarcinomas from neuroendocrine tumors and solid pseudopapillary neoplasms. *Magn Reson Imaging* 2021;**83**:68–76.
21. He M, Song Y, Li H, et al. Histogram analysis comparison of mono-exponential, advanced diffusion-weighted imaging, and dynamic contrast-enhanced MRI for differentiating borderline from malignant epithelial ovarian tumors. *J Magn Reson Imaging* 2020;**52**:257–68.
22. Wu H, Zhang S, Liang C, et al. Intravoxel incoherent motion MRI for the differentiation of benign, intermediate, and malignant solid soft-tissue tumors. *J Magn Reson Imaging* 2017;**46**:1611–8.
23. Lee SK, Jee WH, Jung CK, et al. Multiparametric quantitative analysis of tumor perfusion and diffusion with 3T MRI: differentiation between benign and malignant soft tissue tumors. *Br J Radiol* 2020;**93**:20191035.
24. Chung WJ, Chung HW, Shin MJ, et al. MRI to differentiate benign from malignant soft-tissue tumours of the extremities: a simplified systematic imaging approach using depth, size and heterogeneity of signal intensity. *Br J Radiol* 2012;**85**:e831–6.
25. Li HJ, Cao K, Li XT, et al. A comparative study of mono-exponential and advanced diffusion-weighted imaging in differentiating stage IA endometrial carcinoma from benign endometrial lesions. *J Cancer Res Clin Oncol* 2024;**150**:141.
26. Arslan S, Ergen FB, Aydın GB, et al. Different attenuation models of diffusion-weighted MR imaging for the differentiation of benign and malignant musculoskeletal tumors. *J Magn Reson Imaging* 2022;**55**:594–607.
27. Meng N, Fang T, Feng P, et al. Amide proton transfer-weighted imaging and multiple models diffusion-weighted imaging facilitates preoperative risk stratification of early-stage endometrial carcinoma. *J Magn Reson Imaging* 2021;**54**:1200–11.
28. Zhang J, Chen X, Chen D, et al. Grading and proliferation assessment of diffuse astrocytic tumors with monoexponential, biexponential, and stretched-exponential diffusion-weighted imaging and diffusion kurtosis imaging. *Eur J Radiol* 2018;**109**:188–95.
29. Zhang J, Suo S, Liu G, et al. Comparison of monoexponential, biexponential, stretched-exponential, and kurtosis models of diffusion-weighted imaging in differentiation of renal solid masses. *Korean J Radiol* 2019;**20**:791–800.
30. Zhang K, Dai Y, Liu Y, et al. Soft tissue sarcoma: IVIM and DKI parameters correlate with Ki-67 labeling index on direct comparison of MRI and histopathological slices. *Eur Radiol* 2022;**32**:5659–68.
31. Lim HK, Jee WH, Jung JY, et al. Intravoxel incoherent motion diffusion-weighted MR imaging for differentiation of benign and malignant musculoskeletal tumours at 3 T. *Br J Radiol* 2018;**91**:20170636.
32. Koh DM, Collins DJ, Orton MR, et al. Intravoxel incoherent motion in body diffusion-weighted MRI: reality and challenges. *AJR Am J Roentgenol* 2011;**196**:1351–61.
33. Ogawa M, Kan H, Arai N, et al. Differentiation between malignant and benign musculoskeletal tumors using diffusion kurtosis imaging. *Skeletal Radiol* 2018;**48**:285–92.
34. Noda Y, Goshima S, Fujimoto K, et al. Comparison of the diagnostic value of mono-exponential, Bi-exponential, and stretched exponential signal models in diffusion-weighted MR imaging for differentiating benign and malignant hepatic lesions. *Magn Reson Med Sci* 2021;**20**:69–75.
35. Frei A, Scaglioni MF, Giovanoli P, et al. Definition of the surgical case complexity in the treatment of soft tissue tumors of the extremities and trunk. *Cancers (Basel)* 2022;**14**:1559.